

Macromolecular DCE MRI at 14.1Tesla allows comparative quantitative evaluation of antiangiogenic treatment effects in responsive and resistant GBM models

M. M. Chaumeil¹, S. Rose², S. Sukumar¹, H. Dafni¹, M. Aghi², and S. M. Ronen¹

¹Radiology, University of California San Francisco, San Francisco, CA, United States, ²Neurological Surgery, University of California San Francisco, San Francisco, CA, United States

INTRODUCTION

Glioblastoma (GBM), the most common and aggressive type of primary brain tumors, is also one of the most highly vascularized cancers (1). As a result, antiangiogenic treatment with the anti-VEGF monoclonal antibody Bevacizumab (Avastin; Genentech, CA) is now commonly used in the clinic in conjunction with surgical resection, radio- and chemotherapy. However, many GBM tumors develop resistance to Bevacizumab treatment through mechanisms not fully understood. In an effort to identify indicators of tumor resistance to antiangiogenic treatment, we used macromolecular dynamic contrast-enhanced magnetic resonance imaging (DCE-MRI) (2) at high field (14.1 T) to quantitatively measure the effect of treatment with B20 (a murine Bevacizumab analogue) in two GBM models: one responsive (U87) and one resistant (SF7796, obtained from a patient who developed resistance to Bevacizumab).

MATERIAL & METHODS

Tumor-bearing animals A total of 18 6-weeks-old athymic mice (Nu/Nu homozygous, Simonsen Laboratories, Gilroy, CA) were included in the study. For tumor implantation, animals were anesthetized using ketamine/xylazine (100/20mg.kg⁻¹ respectively) and a suspension of U87 (n=10) or SF7796 (n=8) cells ($\sim 3 \times 10^5$ in 2.5 μ l) was injected into the right caudate-putamen of mice brain (3).

B20 treatment Treated animals (n=5 for U87 group, n=4 for SF7796 group) received an ip injection of B20 (4) twice weekly (5 mg/kg, B20-4.1.1, Genentech, CA) for approx 2 weeks while controls (n=5 for U87, n=4 for SF7796) received the same dose of anti-ragweed antibody (isotype control).

MR system Experiments were performed on a 600 MHz wide bore vertical system ($\varnothing_l=55$ mm) equipped with 100 G.cm⁻¹ imaging gradients (Varian Inc, Palo Alto, CA). Shimming and MR imaging were performed using a Varian millipede ¹H coil ($\varnothing_l=40$ mm, 5cm length).

In vivo MR acquisitions Mice were anesthetized using isoflurane (3% in O₂, 1.5 L.min⁻¹) and a 27G catheter was secured in the tail vein of the animal. Animals were positioned in the magnet using a custom built cradle. MR sessions were performed approx two weeks post B20 treatment initiation. Anatomical imaging was first performed to assess the location of the tumor (coronal SE, TE=20ms, TR=2000ms, FOV=32x32mm, matrix 256x256, slice thickness=0.5mm, gap=0.5mm, Tacq=8min32s, NT=2). Then six 3D gradient echo (GE) pre-contrast images with variable flip angles (FA=2/5/10/30/45/70deg) were acquired successively to determine the R1 maps (TE/TR=1.75/10ms, 4 averages, matrix 128x128x32 FOV=32x20x20mm, slab thickness=20mm, tacq=2m44s). A bolus dose of Albumin-Gd-DTPA (4 μ mol/kg in 200 μ l of PBS, R_i=83.9mM⁻¹.s⁻¹ at 600MHz) (2) was then injected iv through the tail vein catheter and 3D GE post-contrast images (same parameters, FA=45deg) were acquired every 3 min for 45 min.

Post-processing All 3D data sets were zero-filled to 256x256x64. Pixel-by-pixel analysis was performed using MATLAB software (MathWorks, Inc., MA, USA) to generate blood volume fraction (fBV) maps and permeability-surface product (PS, min⁻¹) maps as previously described (2, 5, 6). For each animal, manual segmentation of the tumor region within each slice was performed. Histograms of tumor PS and fBV were then averaged for animals within each of the 4 groups (U87/SF7796 control/treated). Mean \pm sd values of PS and fBV were also calculated for the 4 groups.

RESULTS & DISCUSSION

Figure 1 presents 3D GE pre and post contrast coronal slices, and PS and fBV maps obtained from one animal from each group. Whereas no significant differences were observed prior to treatment, B20 treatment induced a significant decrease in the mean values of PS (PS^{U87}_{Controls}= $4.5 \times 10^{-3} \pm 2.7 \times 10^{-3}$ min⁻¹ vs PS^{U87}_{Treated}= $1.2 \times 10^{-3} \pm 3.4 \times 10^{-4}$ min⁻¹, p=0.03) and fBV (fBV^{U87}_{Controls}= $4.7 \times 10^{-2} \pm 1.4 \times 10^{-2}$ vs. fBV^{U87}_{Treated}= $1.5 \times 10^{-2} \pm 9.6 \times 10^{-4}$, p=0.001) for U87 animals, as illustrated in Figure 1 (upper two rows). In contrast, no significant changes were found between control and treated groups for SF7796 animals, as illustrated in the bottom two rows of Figure 1 (PS^{SF7796}_{Controls}= $2.8 \times 10^{-3} \pm 2.4 \times 10^{-3}$ min⁻¹ vs PS^{SF7796}_{Treated}= $2.5 \times 10^{-3} \pm 1.3 \times 10^{-3}$ min⁻¹, p=0.4 / fBV^{SF7796}_{Controls}= $1.8 \times 10^{-1} \pm 2.1 \times 10^{-1}$ vs. fBV^{SF7796}_{Treated}= $1.1 \times 10^{-1} \pm 9.0 \times 10^{-2}$, p=0.3). Histograms of PS and fBV tumor values averaged throughout animals are presented in Figure 2 for U87 and SF7796 tumor bearing animals. Figures 2.A and 2.C indicate that in U87 tumors B20 treatment induces significant increases in low PS values ($0-4 \times 10^{-4}$ min⁻¹) and low fBV values ($0-7 \times 10^{-3}$) and significant decreases in median range PS values ($1.3-2.7 \times 10^{-4}$ and $3-3.4 \times 10^{-4}$ min⁻¹) and high fBV values ($2.5-5 \times 10^{-2}$). On the other hand, Figures 2.B and 2.D show that in SF7796 tumor bearing animals, B20 treatment did not induce any changes in any of the values both for PS and fBV. The histogram analysis thus provides a visual and quantitative tool to assess heterogeneity of the response to antiangiogenic treatment and confirms the lack of response to B20 in the SF7796 resistant tumor. A parallel survival study showed significantly extended survival in U87 B20 treated animals (93% compared to control), and no increase in survival for SF7796 B20 treated animals (data not shown). In conclusion, this study shows that macromolecular DCE-MRI provides a quantitative assessment of GBM tumor response to antiangiogenic therapy and can distinguish between responsive and resistant tumors at the early stages of treatment.

REFERENCES 1. Chamberlain, Cancer (2010) 2. Dafni et al, MRM (2008) 3. Ozawa et al, In Vivo (2002), 4. Liang, J Biol Chem (2006) 5. Ziv et al, Magn Reson Med (2004) 6. Dafni et al, Neoplasia (2005)

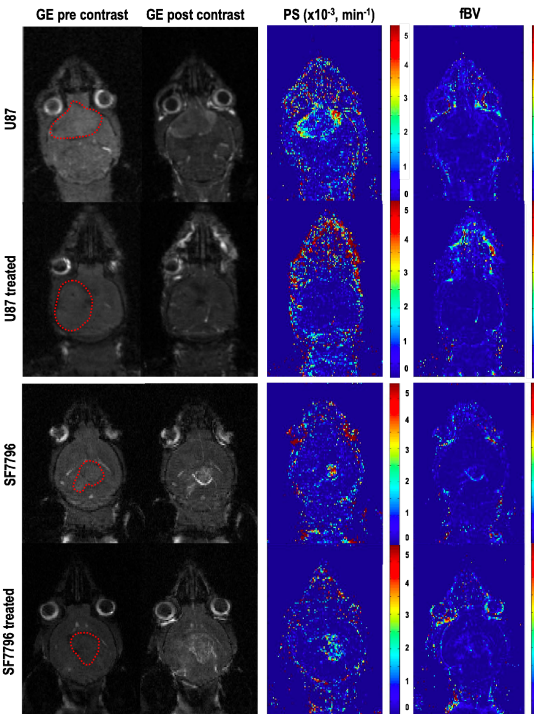


Figure 1 – Coronal slices selected from 3D pre and post contrast GE and corresponding PS and fBV maps for a U87 (upper rows) and a SF7796 (bottom rows) tumor bearing mice. The tumor locations are circled in dashed lines.

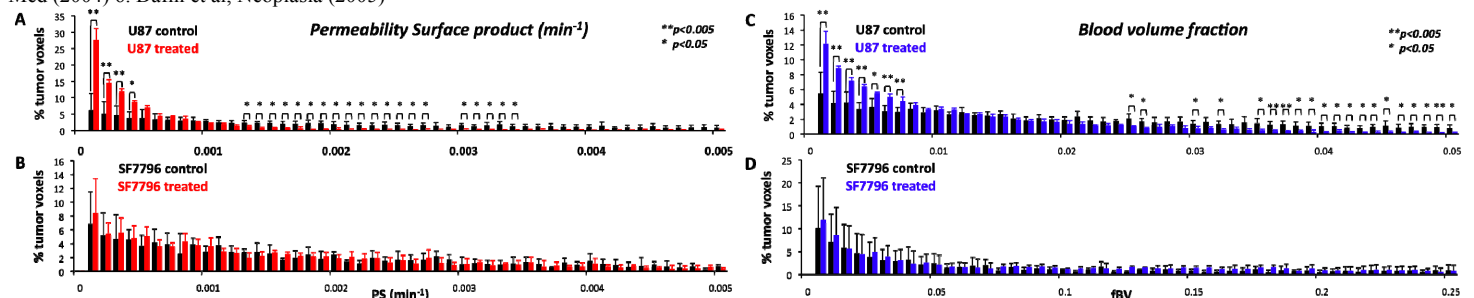


Figure 2 – Averaged histograms of PS (A, B) and fBV (C,D) tumor values for U87 (A,C) and SF7796 (B,D) controls (black) and treated (red PS, blue fBV) animals.